Dynamical Casimir effect in stochastic systems: Photon harvesting through noise

Ricardo Román-Ancheyta,[1,*] Irán Ramos-Prieto,[2] Armando Perez-Leija,[3,4] Kurt Busch,[3,4] and Roberto de J. León-Montiel[5,†]

[1]*Instituto de Ciencias Físicas, Universidad Nacional Autónoma de México, Apartado Postal 48-3, 62251 Cuernavaca, Morelos, México*

[2]*Instituto Nacional de Astrofísica, Óptica y Electrónica, Calle Luis Enrique Erro 1, Santa María Tonantzintla, Puebla Código Postal 72840, México*

[3]*Max-Born-Institut, Max-Born-Straße 2A, 12489 Berlin, Germany*

[4]*Humboldt-Universität zu Berlin, Institut für Physik, AG Theoretische optik Photonik, Newtonstraße 15, 12489 Berlin, Germany*

[5]*Instituto de Ciencias Nucleares, Universidad Nacional Autónoma de México, Apartado Postal 70-543, 04510 Cd. Mx., México*

(Received 5 June 2017; published 1 September 2017)

We theoretically investigate the dynamical Casimir effect in a single-mode cavity endowed with a driven off-resonant mirror. We explore the dynamics of photon generation as a function of the ratio between the cavity mode and the mirror's driving frequency. Interestingly, we find that this ratio defines a threshold—which we referred to as a metal-insulator phase transition—between exponential growth and low photon production. The low photon production is due to Bloch-like oscillations that produce a strong localization of the initial vacuum state, thus preventing higher generation of photons. To break localization of the vacuum state and enhance the photon generation, we impose a dephasing mechanism, based on dynamic disorder, into the driving frequency of the mirror. Additionally, we explore the effects of finite temperature on the photon production. Concurrently, we propose a classical analog of the dynamical Casimir effect in engineered photonic lattices, where the propagation of classical light emulates the photon generation from the quantum vacuum of a single-mode tunable cavity.

DOI: 10.1103/PhysRevA.96.032501

I. INTRODUCTION

One of the most fundamental results of quantum theory is that vacuum space is not really empty. Along these lines, in 1948, Casimir [1] predicted that two parallel mirrors placed in empty space would experience an attractive force as a result of the spatial mismatch between the vacuum modes contained in the cavity and those outside of the mirrors. Remarkably, if the mirrors are allowed to move nonadiabatically, the vacuum mode mismatch may occur in time rather than space. In such a situation, the cavity field does not remain in the vacuum state but gives rise to the generation of photons out of vacuum fluctuations [2,3]. This fascinating phenomenon, termed the dynamical Casimir effect (DCE), can be understood as a parametric amplification of vacuum fluctuations [4–6]. Indeed, it has been shown that a cavity field can be parametrically excited when the cavity length is periodically modulated [7,8]. Particularly in the case where the cavity field is initially in the vacuum state, one can show that its evolution leads to a squeezed vacuum state [9,10], which—unlike a pure vacuum state—contains real photons [11].

To date, several experimental schemes to observe the DCE have been proposed [12–18], but only a few have succeeded [19,20]. The main limitation is because a non-negligible photon production can only be attained when the mirror's speed becomes comparable to the speed of light. Consequently, observations of DCE's represent a very challenging task. Clearly, of importance will be to identify equivalent systems upon which nonadiabatic changes of boundary conditions can be mapped to other physical variables. For instance, in Refs. [19,20], the equivalent action of a quickly moving mirror is mimicked by an inductance variation of a superconducting quantum interference device (SQUID) controlled by a quickly oscillating magnetic flux. Unlike actual mirrors, the inductance of a SQUID can be driven at high frequencies (>10 GHZ), which enables an experimentally detectable photon production.

In this paper, we put forward an experimental setup, based on a semi-infinite waveguide array, in which the propagation of classical light emulates the generation of photons from the quantum vacuum of a single-mode tunable cavity. Using such waveguide configurations, we are able to emulate and explore the dynamics of photon generation as a function of the ratio between the fundamental cavity mode and the driving frequency. Interestingly, through this optical analog, we find a threshold at which the exponentially increasing photon production abruptly drops down. This effect occurs due to the emergence of Bloch-like oscillations that produce strong localization of the initial vacuum state and prevents the generation of photons. In order to break such localization and enhance the photon generation, we propose a dephasing mechanism based on dynamic disorder or noise. Finally, we explore the effects of finite temperature on the photon production and provide a proposal for its implementation.

II. DYNAMICAL CASIMIR EFFECT

We start by considering the effective quantum Hamiltonian describing the dynamics of the electromagnetic field contained in an ideal one-dimensional cavity with a movable mirror, whose position is described by the function $q(t)$ [21,22]:

$$H_{\rm eff}(t) = \sum_k \left\{\omega_k(t) a_k^\dagger a_k + i\,\chi_k(t)\left(a_k^{\dagger 2} - a_k^2\right)\right\} + \sum_{k,j,k\neq j} \frac{i}{2}\mu_{kj}(t)\{a_k^\dagger a_j^\dagger + a_k^\dagger a_j - a_j a_k - a_j^\dagger a_k\}, \tag{1}$$

where a_k and $a_k^\dagger$ are the bosonic operators for the kth field, $\omega_k(t) = k\pi/q(t)$ is the instantaneous cavity frequency, $\chi_k(t) = \dot{\omega}_k(t)[4\omega_k(t)]^{-1}$ is an squeezing coefficient that

*ancheyta6@gmail.com

†roberto.leon@nucleares.unam.mx

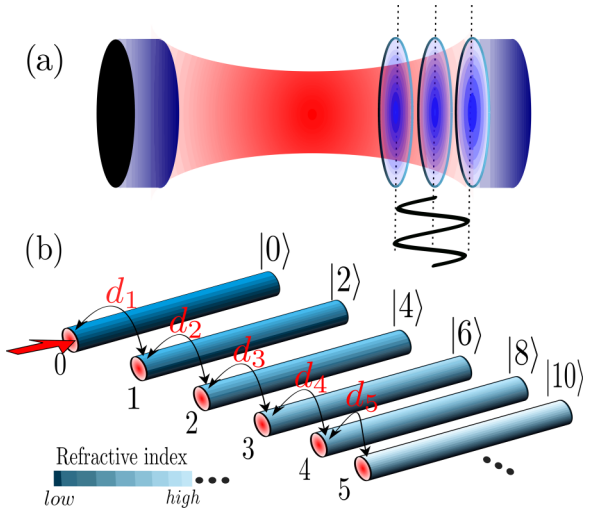

FIG. 1. (a) Schematic representation of a nonstationary optical cavity, in which the dynamical Casimir effect is manifested. (b) Proposed semi-infinite squeezed-like waveguide array for the simulation of photon production from vacuum.

multiplies terms that create photon pairs from vacuum, and $\mu_{kj}(t) = (-1)^{k+j} 2k\sqrt{kj}\dot{q}(t)[(j^2 - k^2)q(t)]^{-1}$ represents the intermode interaction. Here the dot stands for the time derivative, and we have set $\hbar = c = 1$ along with the dielectric permittivity.

To the best of our knowledge, there is no general analytical solution to the corresponding Schrödinger equation for arbitrary $q(t)$ in the above Hamiltonian. As a result, one must perform several approximations to derive a solution. For instance, in Ref. [23], the authors report approximated solutions describing photon generation in cavities endowed with a movable mirror obeying sinusoidal trajectories and a resonance condition, where the mirror's frequency is twice the frequency of some unperturbed cavity mode. In this scenario, the photon generation rate in the fundamental cavity mode rapidly reaches a constant value while the total number of created photons in all modes $\mathcal{N}_{\rm tot} = \sum_{n=1}^{\infty} \mathcal{N}_n$ increases quadratically with time [6], where $\mathcal{N}_n$ is the average photon number in the nth mode.

In what follows, we consider a single-mode cavity [see Fig. 1(a)] such that the intermode interaction term in Eq. (1) vanishes [3]. In this regime, the system is governed by an effective Hamiltonian of the form $H_{\rm eff}(t) \approx \omega(t)a^\dagger a + i\chi(t)(a^{\dagger 2} - a^2)$. Furthermore, we assume a harmonic time-dependent frequency $\omega(t) = \omega_0[1 + \epsilon \sin(\nu t)]$, where ω_0 is the fundamental mode frequency and ϵ and ν are the amplitude and frequency of modulation, respectively. Typically, the amplitude satisfies the condition $\epsilon \ll 1$, so the squeezing parameter can be approximated as $\chi(t) \simeq (\epsilon\nu/4)\cos(\nu t)$ and the cavity frequency becomes $\omega(t) \simeq \omega_0$ [24].

To explore the dynamics of the system in a general, off-resonance regime we take $\nu = 2\omega_0 + K$, with K representing a small frequency shift. This allows us to perform the unitary transformation $T_1 = \exp(-i\nu t a^\dagger a/2)$ and switch to the quasi-interaction picture $H_I = -Ka^\dagger a/2 + i\chi(t)[a^{\dagger 2}\exp(it\nu) - a^2\exp(-it\nu)]$. After applying the rotating-wave approximation, we obtain the time-independent Hamiltonian [24]: $H = (i\epsilon\omega_0/4)(a^{\dagger 2} - a^2) - Ka^\dagger a/2$. Then, we move to a $\pi/4$ rotated frame generated by the transformation $T_2 = \exp(-i\pi a^\dagger a/4)$, which yields

$$\mathcal{H} = -(\epsilon\omega_0/4)(a^{\dagger 2} + a^2) - (K/2)a^\dagger a. \tag{2}$$

Equation (2) represents the simplest effective Hamiltonian for which the photon production in the DCE can exhibit a threshold due to the off-resonance condition provided by the K frequency shift. Now, by inserting $\mathcal{H}$ into the Schrödinger equation, $i\frac{d}{dt}|\Psi(t)\rangle = \mathcal{H}|\Psi(t)\rangle$, and expanding the state vector $|\Psi(t)\rangle$ in terms of Fock states, $|\Psi(t)\rangle = \sum_{m=0}^{\infty} \mathcal{A}_m(t)|m\rangle$, we obtain an infinite set of coupled differential equations for the transition probability amplitudes $\mathcal{A}_m(t)$:

$$i\dot{\mathcal{A}}_m(t) + \lambda_m \mathcal{A}_{m-2}(t) + \lambda_{m+2}\mathcal{A}_{m+2}(t) + Km\mathcal{A}_m(t)/2 = 0, \tag{3}$$

where $\lambda_m = (\epsilon\omega_0/4)\sqrt{m(m-1)}$. The solution of Eq. (3) is given by the matrix elements $\langle m|U(t)|\Psi(0)\rangle = \mathcal{A}_m(t)$, where $U(t) = \exp(-i\mathcal{H}t)$ and $|\Psi(0)\rangle$ is an initial pure state. To compute $U(t)$, it is convenient to disentangle the exponential operator $\exp(-i\mathcal{H}t)$. To do so, we introduce the operators $L_+ = a^{\dagger 2}/2$, $L_- = a^2/2$, and $L_0 = a^\dagger a/2 + 1/4$. Then, by computing the commutators $[L_-, L_+] = 2L_0$ and $[L_0, L_\pm] = \pm L_\pm$, we see that they close an algebra. Consequently, we can split the evolution operator, up to a global phase $e^{-i{\rm Kt}/4}$, as [25] $U(t) = \beta_0^{1/4}\exp(\beta a^{\dagger 2})\exp(a^\dagger a \ln\beta_0)\exp(\beta a^2)$, with $\beta = i\beta_0^{1/2}(1/2\eta)\sinh(\eta\epsilon\omega_0 t/2)$, $\eta = \sqrt{1 - (K/\epsilon\omega_0)^2}$, and $\beta_0 = [\cosh(\eta\epsilon\omega_0 t/2) - i(K/\epsilon\omega_0\eta)\sinh(\eta\epsilon\omega_0 t/2)]^{-2}$. Once we have written the evolution operator as a product of exponentials, we can readily evaluate its action over any initial state.

To estimate the photon production (average photon number) from vacuum, we compute the expectation value $\langle a^\dagger a\rangle_0 = \sum_{m=0}^{\infty} m|\mathcal{A}_m(t)|^2 = \langle 0|U^\dagger(t)a^\dagger a U(t)|0\rangle = -4\beta^2\beta_0^{-1}$, which yields the closed-form expression [26]

$$\langle a^\dagger a\rangle_0 = \sinh^2(\eta\epsilon\omega_0 t/2)/\eta^2. \tag{4}$$

Interestingly, Eq. (4) exhibits three regimes depending on whether the ratio $K/\epsilon\omega_0$ is less, greater, or equal to one. In the case where $K/\epsilon\omega_0 < 1$, the photon generation grows exponentially. This is a pure manifestation of the quantum vacuum fluctuation amplification, which in the particular case of $K = 0$ yields the well-known expression $\langle a^\dagger a\rangle_0|_{K=0} = \sinh^2(\epsilon\omega_0 t/2)$ [13,23]. In contrast, for $K/\epsilon\omega_0 > 1$, the photon production becomes oscillatory, vanishing at $\epsilon\omega_0 t/2 = n\pi/\sqrt{(K/\epsilon\omega_0)^2 - 1}$, with $n \in \mathbb{N}$. Third, at $K/\epsilon\omega_0 = 1$ the photon production is quadratic $\langle a^\dagger a\rangle_0 = (\epsilon\omega_0 t/2)^2$, indicating a threshold between the exponential and the oscillatory behavior. Figure 2 shows a landscape of the photon production $\langle a^\dagger a\rangle_0$ evaluated in the three different regions. The threshold is marked by a dashed line that separates the exponential from the oscillatory behavior. To understand these effects, we explore the spectrum of the system. In particular, for $K/\epsilon\omega_0 > 1$, we see that $\mathcal{H}$ can be diagonalized using the transformation $S(r) = \exp[r(a^{\dagger 2} - a^2)/2]$, with $r = \frac{1}{4}\ln[(K - \epsilon\omega_0)/(K + \epsilon\omega_0)]$. Hence, the transformation $2S^\dagger(r)\mathcal{H}S(r) = -\epsilon\omega_0\sqrt{(K/\epsilon\omega_0)^2 - 1}(a^\dagger a + 1/2) + K/2$ clearly indicates an equally spaced spectrum. This implies

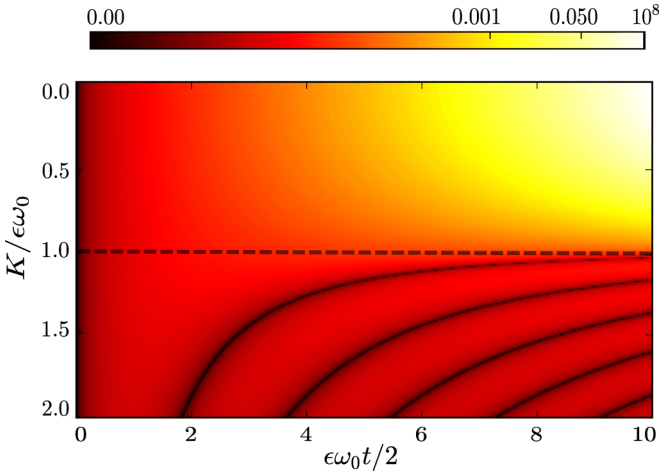

FIG. 2. Photon generation from the vacuum state, $\langle a^\dagger a\rangle_0$, produced by a vibrating cavity. The dashed line indicates the threshold of the system that separates the exponential photon growth (above) from the oscillatory behavior (below). Solid lines show the values where the photon production vanish.

that any initial state is expected to undergo periodic revivals at particular instants given by the zeros of the function describing the photon production (average photon number). As depicted in Fig. 2, the zeros are elucidated by the gaps (dark areas). On the other hand, for $K/\epsilon\omega_0 < 1$ the system exhibits a continuous spectrum which results in a significant photon production. Finally, at the threshold, all the eigenvalues coalesce.

III. SIMULATION OF DCE IN PHOTONIC LATTICES

To translate concepts of the DCE to the optical domain, we map the matrix elements of the $\mathcal{H}$ operator over the interchannel couplings and propagation constants of engineered waveguide arrays; see Fig. 1(b). Within the nearest-neighbor regime, the normalized mode field amplitudes $\{\mathcal{E}_n(z)\}_{n=0}^{\infty}$ are governed by the set of equations [27–30]:

$$id\mathcal{E}_n(z)/dz + \mathcal{C}_n\mathcal{E}_{n-1}(z) + \mathcal{C}_{n+1}\mathcal{E}_{n+1}(z) + \alpha n\mathcal{E}_n(z) = 0, \quad (5)$$

where z represents the propagation distance. To establish a one-to-one connection between the field amplitudes in the waveguide system, Eq. (5), and the probability amplitudes described by Eq. (3), we define the coupling coefficients to be $\mathcal{C}_n = \mathcal{C}_1\sqrt{2n(2n-1)}$, for $n \geqslant 0$, where $\mathcal{C}_1$ stands for the coupling between the zeroth and first waveguide. Moreover, the site energies αn correspond to the waveguide propagation constants obeying a transverse ramped refractive index [31–36]. Notice that in a real waveguide array, the evanescent coupling between sites n and $n-1$, separated by a distance d_n, is given by $C_n = C_1\exp[-(d_n - d_1)/s]$, with d_1 and s being parameters of $\mathcal{C}_1$ that depend on the waveguide width and the associated optical wavelength [30,37].

For the system considered here, the full state-space representation is the harmonic oscillator space divided into even and odd subspaces. However, due to the quadratic nature of $\mathcal{H}$, the equations of motion for the system only connect states with the same parity. Since we are interested in the evolution of the system prepared in the vacuum state (an even state), the waveguide array shown in Fig. 1(b) is the proper one to simulate the dynamics of the DCE, provided that $\mathcal{C}_1 \to \epsilon\omega_0/4$ and $\alpha \to K/2$, with z playing the role of time. Under these premises, Eq. (5) and the even terms of Eq. (3) are equivalent. Conversely, to simulate the odd terms of Eq. (3), one would require an independent photonic lattice. Indeed, the full system could be simulated by designing both arrays, one on top of the other, with a sufficient separation to neglect possible interactions between them [28].

To perform the DCE's photonic simulation, we excite the first waveguide ($|0\rangle$ state). Accordingly, the field amplitude at site m, $\mathcal{E}_m(z)$, can be obtained by writing $\mathcal{E}_m(z) = \langle 2m|U(z)|0\rangle$. One can then find that the intensity at the mth waveguide is

$$I_m(z) = |\mathcal{E}_m(z)|^2 = \frac{(2m)!}{(2^m m!)^2}\frac{\langle a^\dagger a\rangle_0^m}{(1+\langle a^\dagger a\rangle_0)^{m+\frac{1}{2}}}, \quad (6)$$

which resembles the probability distribution for a thermal state. In this optical context, *the photon production* $\langle a^\dagger a\rangle_0$ can be expressed as $\langle a^\dagger a\rangle_0 = \sinh^2(2C_1 z\eta_x)\eta_x^{-2}$, with $\eta_x^2 = 1 - x^2$ and $x = \alpha/2C_1$. Alternatively, one can write the photon production in terms of the intensity at the mth waveguide as $\langle a^\dagger a\rangle_0^{\text{clas}} = 2\sum_{m=0}^{N} m I_m(z)$. This last expression constitutes the classical analog of photon generation from the vacuum state at a distance z, where the factor 2 comes from considering only the even states, and N is the maximum number of waveguides.

Figure 3 shows the intensity distributions $I_m(z)$ for two waveguide arrays—designed using realistic experimental parameters [31,38]—above and below the threshold. For $x < 1$

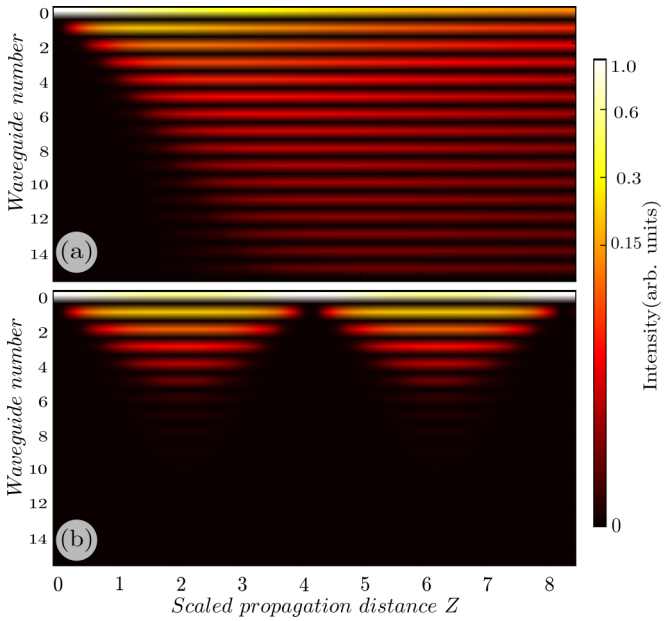

FIG. 3. Light propagation in the waveguide array depicted in Fig. 1(b), as a function of the scaled propagation distance Z (see main text for details), when the first site (vacuum state) is initially excited; ramping constant $\alpha = 0.5\,\text{cm}^{-1}$. (a) Extended propagation of the initial excitation (metal phase) with $C_1 = 0.26\,\text{cm}^{-1}$. (b) Localization of the excitation (insulator phase) with $C_1 = 0.2\,\text{cm}^{-1}$.

[Fig. 3(a)], the propagation of the initial excitation, as a function of the scaled distance $Z = 2C_1 z$, shows a rapid delocalization throughout the array. In contrast, for $x > 1$ [Fig. 3(b)] the system spectrum forms a Wannier-Stark ladder [38], causing spatial mode localization, giving rise to Bloch-like revivals at $Z_{\rm rev} = n\pi/\sqrt{x^2-1}$. Indeed, such localization effects can be understood by noticing that the condition $x > 1$ implies that $\alpha > 2C_1$. Physically, this entails that the transition amplitudes propagate under the influence of a ramping potential, sloped by the parameter α, which produces an equidistant Bloch-like spectrum that ultimately leads to localization of the vacuum state [39].

Interestingly, the spectral changes between an extended and localized excitation resemble a kind of metal-insulator phase transition [28], with a threshold at $x = 1$. In that sense, Fig. 3(a) shows the dynamics of the system in the metal phase, while Fig. 3(b) illustrates the insulator phase. Importantly, it should be stressed that photons produced in the metallic phase of the DCE can be easily detected, while their corresponding observation in the insulator phase is very challenging. Therefore, it is of interest to envision new approaches that may allow us to access the insulator phase of the DCE.

IV. ENHANCING PHOTON PRODUCTION THROUGH NOISE

As discussed above, when the DCE system is at the *insulator phase*, the initial excitation remains localized around the first waveguide, i.e., the vacuum state. This results in a low photon production that could be measured only at very specific distances. To overcome this situation, we introduce a pure-dephasing mechanism, which simulates the effect of a Markovian environment interacting with the photonic system. This interaction results in the delocalization of the excitation, thus leading to an enhancement of photon production, a phenomenon called environment-assisted quantum transport [40–46]. Indeed, to implement such mechanism in a waveguide array, one needs to include Gaussian fluctuations in the propagation constant of individual waveguides. This can be experimentally implemented by randomly changing the speed at which each waveguide is inscribed; see Refs. [47,48] for details on the fabrication of such system. Remarkably, in the context of a non-stationary cavity field mode, this phenomenon could be observed by adding stochastic fluctuations to the frequency shift K.

Under different considerations over the random fluctuations, it entails to consider a pure-dephasing process for the field density operator ρ [40,49,50]. Thus, we can study the action on ρ of the generator $D[x]$ defined in the Lindblad form as $D[x]\rho = x\rho x^\dagger - (x^\dagger x\rho + \rho x^\dagger x)/2$, for which the master equation to solve takes the form $\dot\rho = -i[\mathcal{H},\rho] + \gamma D[a^\dagger a]\rho$, where γ is the dephasing rate. By inspecting the term $\langle n|D[a^\dagger a]\rho|m\rangle = -(n-m)^2\rho_{n,m}/2$, we can see that only the nondiagonal elements of the density matrix are directly affected by the random fluctuations, a footprint of the pure-dephasing process.

We now compute the average value of the number and quadratic field operators. From the master equation, one can obtain the corresponding equations of motion: $d\langle a^\dagger a\rangle/d\tau = i(\langle a^{\dagger 2}\rangle - \langle a^2\rangle)$, $d\langle a^2\rangle/d\tau = 2\tilde K_\gamma\langle a^2\rangle + i(2\langle a^\dagger a\rangle + 1)$, and $d\langle a^{\dagger 2}\rangle/d\tau = d\langle a^2\rangle^*/d\tau$, where $\tau = \epsilon\omega_0 t/2$ and $\tilde K_\gamma = iK/\epsilon\omega_0 - 2\gamma/\epsilon\omega_0$. By considering the initial conditions $\langle a^\dagger a\rangle|_{\tau=0} = \langle a^2\rangle|_{\tau=0} = \langle a^{\dagger 2}\rangle|_{\tau=0} = 0$, we have numerically solved the above equations of motion using the QUTIP package [51].

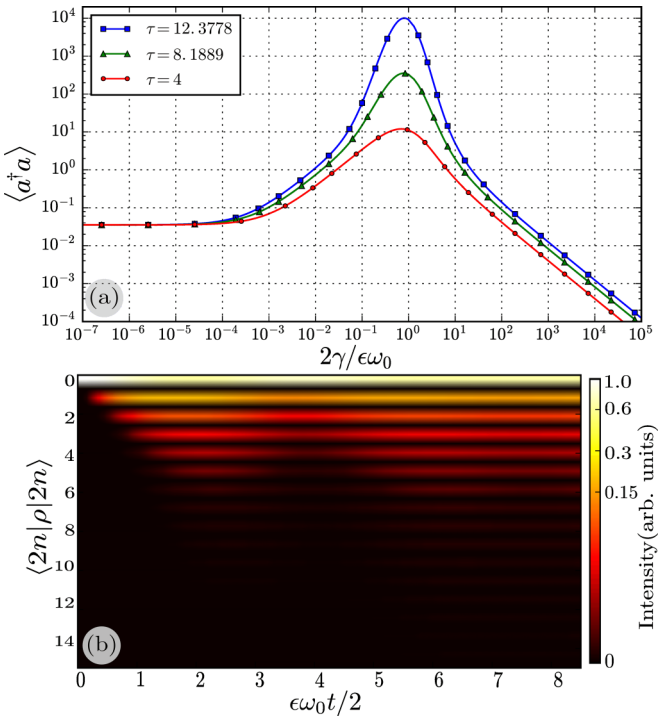

FIG. 4. (a) Enhancement of photon generation as a function of the scaled dephasing rate, $2\gamma/\epsilon\omega_0$, at three revival times. (b) Evolution of the diagonal elements of the system's density matrix with $2\gamma/\epsilon\omega_0 = 0.04$.

Figure 4(a) shows the photon production $\langle a^\dagger a\rangle$ as a function of the dephasing rate when the system is in the insulator phase (Bloch oscillator phase) at the specific time where, in the absence of dephasing, the photon production is minimum (that is, at the Bloch period). For the case when the dephasing is weak, or simply absent, the refractive index of the waveguides are essentially unaffected and Bloch-like oscillations occur. However, by moderately increasing the dephasing rate, one can see that the Bloch-like oscillations cease to exist, Fig. 4(b), resulting in the enhancement of the photon production rate. The mechanism behind such photon enhancement is that moderate dephasing breaks the regular equidistant eigenspectrum and as a result it prevents the manifestation of Bloch oscillations. To better illustrate the effects of dephasing, in Fig. 4(b) we monitor the diagonal elements of the density matrix, $\langle 2n|\rho|2n\rangle$, as a function of time. Owing to the interaction of the system with an environment, the delocalization from the first site is broken, thus inducing a larger contribution to the photon generation. Notice that delocalization is more dramatic at the Bloch-like revival regions, that is, in points where the photon production is zero in the absence of dephasing. Finally, for strong dephasing rates, cross-interference terms between different sites are completely erased and the state of pure diffusive propagation—where the probability of the excitation to remain in its initial state is maximum—is reached [52].

V. DCE AT FINITE TEMPERATURE

Another mechanism for the enhancement of photon production considers thermal effects on the creation of photons. To include thermal effects in our system, we make use of the Hamiltonian in Eq. (2) to write the average photon number evolution for an initial thermal field $\rho_{\rm th}(0) = \sum_{n=0}^{\infty} P_n |n\rangle\langle n|$, where $P_n = \bar{n}_{\rm th}^n/(1+\bar{n}_{\rm th})^{n+1}$, and $\bar{n}_{\rm th} = 1/(\exp(\hbar\omega/k_B T) - 1)$,

$$\langle a^\dagger a\rangle_{\rm th} = \sum_{n=0}^{\infty} P_n \langle a^\dagger a\rangle_n = (1+2\bar{n}_{\rm th})\langle a^\dagger a\rangle_0 + \bar{n}_{\rm th}. \quad (7)$$

Here $\langle a^\dagger a\rangle_n = \langle n|U^\dagger(z) a^\dagger a U(z)|n\rangle = (1+2n)\langle a^\dagger a\rangle_0 + n$ stands for the photon production from an initial Fock state $|n\rangle$. Notice that Eq. (7) predicts an enhancement of photon production that depends on the average photon number of the thermal field. In the photonic context, a thermal field could be designed by making use of an independent disordered waveguide array, where an initially injected coherent state is thermalized [53]. Because the implementation of both systems relies on the same integrated-optics technology, they could be designed in tandem, so the losses in the coupling of the thermal state to our proposed system would be negligible.

VI. CONCLUSIONS

In this work we have proposed a photonic system for the classical simulation of the dynamical Casimir effect. We showed that photon generation from the vacuum state may exhibit a transition from an exponential growth to an oscillatory behavior, thus resembling a metal-insulator phase transition. Furthermore, we found that the insulator phase appears as a result of the Bloch-like oscillations in the dynamics of the system. This causes a strong localization of the initial excitation in the first waveguide, leading to a poor contribution to the Casimir-like radiation. To overcome this situation, we discussed two possible solutions. First, we made use of a dephasing mechanism in which the coherent evolution of the system is broken by means of its interaction with a Markovian environment. The reduced coherence of the system causes a delocalization of the excitation, thus increasing the photon production by up to two orders of magnitude in the first Bloch-like revival. In the second mechanism, based on considering thermal effects in the DCE, we showed that in this case the photon production is enhanced by a factor that depends on the average photon number of the thermal field that is initially injected in the system. Finally, we would like to point out that DCE modifications due to Kerr nonlinearities, recently predicted in Ref. [9], could also be tested in our proposed photonic system by changing the linear refractive index profile to a quadratic one.

ACKNOWLEDGMENTS

R.R.-A. thanks CONACYT, Mexico, for Scholarship No. 379732 and Project No. 166961, and DGAPA-UNAM, México, for support under Project No. IN113016. A.P.-L. and K.B. acknowledge financial support by the Deutsche Forschungsgemeinschaft (DFG) within project BU 1107/10-1 of the Priority Program SPP 1839 Tailored Disorder. R.J.L.-M. thankfully acknowledges the computer resources, technical expertise, and support provided by the Laboratorio Nacional de Supercómputo del Sureste de México, CONACYT network of national laboratories.

[1] H. B. G. Casimir, Proc. K. Ned. Akad. Wet. B **51**, 793 (1948).
[2] G. T. Moore, J. Math. Phys. **11**, 2679 (1970).
[3] P. D. Nation, J. R. Johansson, M. P. Blencowe, and F. Nori, Rev. Mod. Phys. **84**, 1 (2012).
[4] E. Yablonovitch, Phys. Rev. Lett. **62**, 1742 (1989).
[5] J. Schwinger, Proc. Natl. Acad. Sci USA **89**, 4091 (1992).
[6] V. V. Dodonov, Phys. Scripta **82**, 038105 (2010).
[7] R. Román-Ancheyta, M. Berrondo, and J. Récamier, J. Opt. Soc. Am. B **32**, 1651 (2015).
[8] R. de J. León-Montiel and H. M. Moya-Cessa, J. Opt. **17**, 065202 (2015).
[9] R. Román-Ancheyta, C. González-Gutiérrez, and J. Récamier, J. Opt. Soc. Am. B **34**, 1170 (2017).
[10] E. Giacobino and C. Fabre, Appl. Phys. B **55**, 189 (1992).
[11] G. Breitenbach, S. Schiller, and J. Mlynek, Nature (London) **387**, 471 (1997).
[12] A. Lambrecht, M.-T. Jaekel, and S. Reynaud, Phys. Rev. Lett. **77**, 615 (1996).
[13] M. Uhlmann, G. Plunien, R. Schützhold, and G. Soff, Phys. Rev. Lett **93**, 193601 (2004).
[14] C. Braggio, G. Bressi, G. Carugno, C. D. Noce, G. Galeazzi, A. Lombardi, A. Palmieri, G. Ruoso, and D. Zanello, Europhys. Lett. **70**, 754 (2005).
[15] W.-J. Kim, J. H. Brownell, and R. Onofrio, Phys. Rev. Lett. **96**, 200402 (2006).
[16] S. De Liberato, C. Ciuti, and I. Carusotto, Phys. Rev. Lett. **98**, 103602 (2007).
[17] J. R. Johansson, G. Johansson, C. M. Wilson, and F. Nori, Phys. Rev. Lett. **103**, 147003 (2009).
[18] C. M. Wilson, T. Duty, M. Sandberg, F. Persson, V. Shumeiko, and P. Delsing, Phys. Rev. Lett. **105**, 233907 (2010).
[19] C. M. Wilson, G. Johansson, A. Pourkabirian, M. Simoen, J. R. Johansson, T. Duty, F. Nori, and P. Delsing, Nature (London) **479**, 376 (2011).
[20] P. Lähteenmäki, G. S. Paraoanu, J. Hassel, and P. J. Hakonen, Proc. Natl. Acad. Sci. **110**, 4234 (2013).
[21] C. K. Law, Phys. Rev. A **49**, 433 (1994).
[22] R. Schützhold, G. Plunien, and G. Soff, Phys. Rev. A **57**, 2311 (1998).
[23] V. V. Dodonov and A. B. Klimov, Phys. Rev. A **53**, 2664 (1996).
[24] A. V. Dodonov and V. V. Dodonov, Phys. Rev. A **85**, 015805 (2012).
[25] M. Ban, J. Opt. Soc. Am. B **10**, 1347 (1993).
[26] A. V. Dodonov and V. V. Dodonov, Phys. Scripta **2013**, 014017 (2013).
[27] A. A. Sukhorukov, A. S. Solntsev, and J. E. Sipe, Phys. Rev. A **87**, 053823 (2013).
[28] M. K. Nezhad, A. R. Bahrampour, M. Golshani, S. M. Mahdavi, and A. Langari, Phys. Rev. A **88**, 023801 (2013).

[29] A. Perez-Leija, H. Moya-Cessa, A. Szameit, and D. N. Christodoulides, Opt. Lett. **35**, 2409 (2010).
[30] R. Keil, A. Perez-Leija, F. Dreisow, M. Heinrich, H. Moya-Cessa, S. Nolte, D. N. Christodoulides, and A. Szameit, Phys. Rev. Lett. **107**, 103601 (2011).
[31] R. Keil, A. Perez-Leija, P. Aleahmad, H. Moya-Cessa, S. Nolte, D. N. Christodoulides, and A. Szameit, Opt. Lett. **37**, 3801 (2012).
[32] T. Pertsch, P. Dannberg, W. Elflein, A. Brauer, and F. Lederer, Phys. Rev. Lett. **83**, 4752 (1999).
[33] R. Morandotti, U. Peschel, J. S. Aitchison, H. S. Eisenberg, and Y. Silberberg, Phys. Rev. Lett. **83**, 4756 (1999).
[34] S. Longhi, Phys. Rev. Lett. **101**, 193902 (2008).
[35] M. Lebugle, M. Grafe, R. Heilmann, A. Perez-Leija, S. Nolte, and A. Szameit, Nat. Commun. **6**, 8273 (2015).
[36] K. Wang, S. Weimann, S. Nolte, A. Perez-Leija, and A. Szameit, Opt. Lett. **41**, 1889 (2016).
[37] A. Szameit and S. Nolte, J. Phys. B **43**, 163001 (2010).
[38] S. Stutzer, A. S. Solntsev, S. Nolte, A. A. Sukhorukov, and A. Szameit, APL Photon. **2**, 051302 (2017).
[39] S. Stutzer, Y. V. Kartashov, V. A. Vysloukh, V. V. Konotop, S. Nolte, L. Torner, and A. Szameit, Opt. Lett. **38**, 1488 (2013).
[40] P. Rebentrost, M. Mohseni, I. Kassal, S. Lloyd, and A. Aspuru-Guzik, New J. Phys. **11**, 033003 (2009).
[41] M. Plenio and S. Huelga, New J. Phys. **10**, 113019 (2008).
[42] R. de J. León-Montiel, I. Kassal, and J. P. Torres, J. Phys. Chem. B **118**, 10588 (2014).
[43] S. Viciani, M. Lima, M. Bellini, and F. Caruso, Phys. Rev. Lett. **115**, 083601 (2015).
[44] R. de J. León-Montiel, M. A. Quiroz-Juárez, R. Quintero-Torres, J. L. Domínguez-Juárez, H. M. Moya-Cessa, J. P. Torres, and J. L. Aragón, Sci. Rep. **5**, 17339 (2015).
[45] D. N. Biggerstaff, R. Heilmann, A. A. Zecevik, M. Gräfe, M. A. Broome, A. Fedrizzi, S. Nolte, A. Szameit, A. G. White, and I. Kassal, Nat. Commun. **7**, 11282 (2016).
[46] R. de J. León-Montiel and P. A. Quinto-Su, Sci. Rep. **7**, 44287 (2017).
[47] F. Caruso, A. Crespi, A. G. Ciriolo, F. Sciarrino, and R. Osellame, Nat. Commun. **7**, 11682 (2016).
[48] D. Guzman-Silva, R. de J. León-Montiel, M. Heinrich, J. P. Torres, H. Moya-Cessa, M. Graefe, A. Perez-Leija, and A. Szameit, in *Conference on Lasers and Electro-Optics*, OSA Technical Digest (online) (Optical Society of America, 2016), paper FTh1A.8.
[49] A. Eisfeld and J. S. Briggs, Phys. Rev. E **85**, 046118 (2012).
[50] R. de J. León-Montiel and J. P. Torres, Phys. Rev. Lett. **110**, 218101 (2013).
[51] J. Johansson, P. Nation, and F. Nori, Comp. Phys. Commun. **184**, 1234 (2013).
[52] V. Kendon, Math. Struct. Com. Sci. **17**, 1169 (2006).
[53] H. E. Kondakci, A. F. Abouraddy, and B. E. A. Saleh, Nat. Phys. **11**, 930 (2015).